Mg^{2+} and Ca^{2+} were still mainly existed in coarse particles, the concentration increased with particle size, but which obviously lower than other seasons. The reasons may be as follows: the average precipitation in autumn of 2014 in Chongqing was twice than previous years, the sunshine hours were less, and the relative humidity was higher (RH=82.97%), the wet deposition process has a certain scavenging effect on the dust in the air through it. Besides, the wind speed (1.21 $m \cdot s^{-1}$) in autumn was low, which was not conducive to the diffusion of dust into the air, these may be the main reasons why the concentration of Mg^{2+} and Ca^{2+} were lower in autumn, but higher in other seasons.

3.3.2 *The size distribution of secondary ions*

Fig. 4(d) showed particle size distributions of SNA (SO_4^{2-}, NH_4^+ and NO_3^-), all appeared a single-peak distribution, but peaks were not exactly the same.

SO_4^{2-} mainly distributed in the droplet mode with a peak at the range of 0.65-2.10 μm, elevated a grain level when compared with that in summer. As shown in Table 1, the mole ratio of sulfate at the range of 0.65~2.10 μm to SO_2 was about 0.26, the highest relative humidity (RH=82.97%) and less sunshine hours in autumn (121.1), indicating that in-cloud formation of sulfate may be important in sulfate formation.

$NH_4^+$and NO_3^- mainly existed at the range of 0.65-1.10 μm in the droplet mode, their correlation was great (r=0.81). NH_4^+ and NO_3^- in the fine mode mainly existed in the form of NH_4NO_3, which was similar to that in spring and summer.

3.4 *The particle size distributions of water-soluble Ions in autumn*

3.4.1 *The size distribution of primary ions*

The particle size distributions of various water-soluble ions in autumn, in terms of the aerodynamic diameter, are shown in Fig. 5(a)-(d).

Fig. 5

Fig. 5 showed particle size distributions of K^+ and Cl^- were almost same, both were a single-peak distribution, with the peak at range of 0.65~1.10 μm, indicated that the relationships of two ions are close (r=0.80). During the Spring Festival in Chongqing, due to the firecrackers, fireworks and biomass burning, a large amount of chlorine generated and entered the aerosol. At this moment, Cl^- will be mainly combined with K^+ in the form of KCl.

Na^+ was a double peak type, and the peak concentrations appeared in the particle size ranges of 0.65-1.10 μm and 5.80-9.00 μm. The Ca^{2+} peak value of the coarse mode in winter was higher than other seasons, indicating that there were more crust sources in that season (Liu et al., 2017). The concentrations of Mg^{2+} and F^- were low in each particle, and principal appeared in coarse mode.

3.4.2 *The size distribution of primary ions*

Fig. 5 showed particle size distributions of SNA (SO_4^{2-}, NO_3^- and NH_4^+) were almost same, all showed a unimodal distribution, with peaks all at range of 0.65-1.10 μm, indicating that the relationships of three ions are close (R_{SA}=0.96, R_{NA}=0.92, R_{SN}=0.84).

SO_4^{2-} mainly distributed in the droplet mode. Due to the fact that the precipitation was only 49.5 mm in winter, and the sunshine hours was also less, SO_4^{2-} could attributed to non-precipitation reactions in cloud droplets or droplets. Because average temperature was very low compared with other seasons, NH_4^+ and NO_3^- in the fine mode mainly existed in the form of NH_4NO_3, which was similar to spring. In addition, $\rho(NO_3^-)$ in winter was significantly higher than other seasons from Fig. 5, it may be due to the fact that the particulate NO_3^- was mainly composed of volatile components, it was susceptible to winter temperatures, so relatively low temperature and higher NO_x emissions were beneficial to the formation of NO_3^- in aerosols (Zhang et al., 2011). At the same time, the atmosphere structure of Beibei urban area was more stable in winter, the inversion temperature was significant, which contributed to the transformation of SNA, and then it led to higher concentration in winter.

3.5 *Balance and correlation of ions*

The acidity-alkalinity of atmospheric aerosols has an important effect on the pH of precipitation, which may cause precipitation acidification, or may cause acidity of precipitation plays a neutralization role (Tang et al., 2005). Some studies showed that NO_3^-, SO_4^{2-}, F^- and Cl^- are favorable for the acidity of aerosol, whereas NH_4^+, K^+, Na^+, Mg^{2+} and Ca^{2+} increase the pH of aerosol (Xu et al., 2012). The ion balance is a good indicator to study the acidity of aerosol, which is determined by both anion equivalents (AE) and cation equivalents (CE) calculated with the following equations:

$$\text{AE(Anion equivalent)}=\frac{\rho(F^-)}{19}+\frac{\rho(Cl^-)}{35.5}+\frac{\rho(NO_3^-)}{62}+\frac{\rho(SO_4^{2-})}{48} \quad (1)$$

$$\text{CE(Cation equivalent)}=\frac{\rho(Na^+)}{23}+\frac{\rho(NH_4^+)}{18}+\frac{\rho(K^+)}{39}+\frac{\rho(Mg^{2+})}{12}+\frac{\rho(Ca^{2+})}{20} \quad (2)$$

On the one hand, the correlation analysis between ions can reveal the binding modes of ions in aerosol; on the other hand, it can infer the origin of the material. In this paper, the correlations among nine kinds of water-soluble ions in $PM_{2.1}$ and $PM_{9.0}$ were compared. The correlation coefficients between different ions were summarized in Table 2 and Table 3.

Table 2

Table 3

As Table 2 and Table 3 showed, the correlation between the anions and cations were significant, indicating that the measured data was valid. The ratio of AE/CE in $PM_{2.1}$ was 0.67 while the ratio of $PM_{9.0}$ was 0.49, and the total cation concentration was distinctly higher than that of anion, namely, the anions from the aerosol in this area were relatively depleted. This finding markedly differed from the results in Jinyun Mountain area from January 2005 to May 2006 (He et al., 2012), where the total anions concentration in TSP was higher than the cations concentration. These differences were large because of the significant increase in Ca^{2+} concentration caused by growing urban construction, road dust; It may also be the excess NH_4^+ compared with previous years (Jiang et al. 2009; He et al.,2012), especially the existence of alkaline NH_4^+ (Satsangi et al., 2013).

The correlation between SNA was significant in both $PM_{2.1}$ and $PM_{9.0}$ ($r \geq 0.75$), indicating that they may have the same secondary transformation source; Meanwhile, the correlation between the two secondary ions NH_4^+ and NO_3^- in $PM_{2.1}$ was far more significant, suggesting that they mainly existed in the form of NH_4NO_3 in the fine particles. Ca^{2+} and Mg^{2+} had significant correlation in $PM_{2.1}$, but were poorly related to other ions which indicated that Ca^{2+} and Mg^{2+} may have the same source. The result of Na^+ varied greatly among different particles, Na^+ showed a significant correlation with Cl^-, NO_3^-, SO_4^{2-} in $PM_{2.1}$, but was only significantly related with SO_4^{2-} in $PM_{9.0}$ ($P<0.05$), indicating that Na^+ in the fine particles may exist in various forms such as NaCl, $NaNO_3$ and Na_2SO_4; However, in the coarse particles, the sodium salt was mainly in the form of Na_2SO_4. Cl^- had a low correlation with Na^+ in $PM_{9.0}$, but had strong correlation with other ions, indicating that the source of two ions were different, and Beibei is located in inland, so it can exclude Cl^- and Na^+ with marine sources. The correlation coefficients of K^+ and NH_4^+ in $PM_{2.1}$ and $PM_{9.0}$ were significantly correlated ($r>0.50$), indicating that these

two might have the same sources, and it also verified the phenomenon earlier that K^+ and NH_4^+ had a similar seasonal variation trend. F^- had a strong correlation with SO_4^{2-} in $PM_{2.1}$, indicating that F^- in fine particles may have the same origin as SO_4^{2-}.

In general, the correlations between Na^+, NH_4^+, K^+, Cl^-, NO_3^-, SO_4^{2-} and total water-soluble ions (Σ(-) and Σ(+)) were stronger in $PM_{2.1}$, but the correlations between Mg^{2+}, Ca^{2+}, F^- and total water-soluble ions were stronger in $PM_{9.0}$. This verified the previous reports that Na^+, NH_4^+, K^+, Cl^-, NO_3^-, SO_4^{2-} mainly presented in fine particles, and Mg^{2+}, Ca^{2+}, F^- mainly presented in coarse particles.

3.6 *Principal component analysis of water soluble ions in aerosols*

In order to better explore the main sources of water-soluble ions in aerosols in Beibei Suburb, the principal component analysis (PCA) was used to classify and analyze 9 kinds of water-soluble ions in $PM_{2.1}$ and $PM_{9.0}$ (Satsangi et al., 2013). Factor analysis results were summarized in Table 4.

Table 4

For $PM_{2.1}$, two major factors contributing to a larger variance contribution were screened, and 62.53% of the water-soluble ion sources were explained. Among the factors 1, NH_4^+, NO_3^-, SO_4^{2-}, Cl^- and K^+ played a significant role, and their load coefficients were more than 0.70. SNA mainly came from the secondary transformation of gaseous precursor; $C1^-$ and K^+ were mainly derived from combustion process, indicating that factors 1 mainly refers to the secondary transformation process of anthropogenic pollutants and combustion source. The effects of Ca^{2+}, Mg^{2+} and F^- were significant in factors 2, and their load coefficients reached to more than 0.50. Ca^{2+} is the identification element of building materials, and Ca^{2+} and Mg^{2+} in aerosol mainly come from building, road dust and soil particle. Therefore, factors 2 mainly refers to dust and soil sources.

For $PM_{9.0}$, three main factors contributing to a larger variance contribution were screened, explaining 76.01% of the source of water soluble ions. Among the factors 1, SNA played a significant role, and their load coefficients were more than 0.80, indicating that factors 1 mainly refers to the secondary transformation process of anthropogenic pollution sources. In factors 2, the effects of Ca^{2+} and Mg^{2+} were significant, and the results were similar to the analysis result of factors 2 for $PM_{2.1}$. In factors 3, only Na^+ had a very significant effect, and its load coefficient

was up to 0.89. Part of Na^+ came from marine source, coexisting with Cl^-, and the other was mainly related to soils and dust. Beibei Suburb in Chongqing is located in inland areas, Na^+ mainly derived from soil. Therefore, the factors 3 may be the soil source, and the factors 2 may be the dust from building construction and road construction.

The results of principal component analysis showed that the contribution rate of factors 1 in $PM_{2.1}$ and $PM_{9.0}$ was much higher than that of other factors, which indicates that water soluble ions in aerosol from Beibei mainly come from vehicle exhaust emissions, fossil fuel and biomass fuel combustion. And maximum load factor in factors 1 was SNA, showed that the secondary ions produced by NH_3 (anthropogenic and natural sources), NO_x and SO_2 (emitted from fuel combustion) under certain meteorological conditions are the most important sources of water-soluble ions. What's more, the dust caused by soils and road construction also contributed to the production of water-soluble ions.

3.7 Formation mechanism of sulfate and nitrate in different particle sizes

To investigate the extent to which SO_2 converted to SO_4^{2-} and NO_2 converted to NO_3^-, sulfur oxidation ratios (SOR) and nitrogen oxidation ratios (NOR) were calculated, which can clearly indicate secondary transformation processes (Behera and Sharma, 2010). These two conversion ratios are defined as follows (Cheng et al., 2011):

$$SOR = \frac{[SO_4^{2-}]}{[SO_4^{2-}]+[SO_2]} \quad (1)$$

$$NOR = \frac{[NO_3^-]}{[NO_3^-]+[NO_2]} \quad (2)$$

Fig. 6

Size distributions of apparent conversion rate (SOR and NOR) in each season, plotted in Fig. 6. Many studies found that higher SOR and NOR values imply that the photochemical oxidation of precursor gases has led to the formation of larger proportions of sulfate- and nitrate-containing secondary aerosol particles (Sun et al., 2006; Wang et al., 2005). Ohta et al. (1990) identified, it would occur the transformation from SO_2 in the atmosphere when SOR> 0.10. As shown in Fig. 6, SOR values over four seasons were greater than 0.10 in the fine particles and lower than 0.10 in the coarse particles, which indicated the conversion of SO_2 mostly occurs in the fine particles. SOR was the highest in summer and lowest in winter, it implied stronger

436 photochemical reaction of SO_2 in summer, meanwhile, it could more conducive to secondary
437 conversion of SO_2 with higher temperature, relative humidity and O_3 concentration. More
438 remarkably, SOR value of condensation-mode (0.43-0.65 μm) was greater than 0.10 only in
439 summer unlike as other seasons. It explained that SO_4^{2-} was mainly from the oxidation of SO_2
440 with subsequent hygroscopic growth, corresponding with the previous discussion (3.2.2). SOR
441 values were slightly larger than 0.10 in spring and autumn in ranges of 0.65-1.10 μm and
442 0.65-2.10, respectively, implying that photochemical oxidation of SO_2 was not the main process.
443 SOR values were all less than 0.10 in each particle in winter, while SO_4^{2-} concentration was the
444 highest, secondary conversion efficiency of SO_2 in winter was much lower than other seasons.
445 Higher SO_4^{2-} accompanied lower SOR indicated that the sources might mainly come from the
446 long range transportation, leading to the heterogeneous reaction of SO_2 (Wu et al., 2016).
447 As showed in Fig. 6, NOR values of fine-mode over four seasons were greater than those in
448 coarse-mode, indicating that the conversion of NO_2 mostly occurred in the fine particles. NOR
449 values were lower than 0.10 in all particles, implying that the oxidation ratios of nitrogen existed
450 at a very low level. NOR values in winter were significantly higher than other seasons and had
451 great correlation with SOR in the fine particles. NOR in summer was the lowest that probably
452 caused by temperature. The volatile NH_4NO_3 could be decomposed into NH_3 and HNO_3 at high
453 temperature that might lead to the lower NOR (Suzuki et al., 2008). What's more, high
454 temperature and high photochemical reaction in summer, could not only conducive to the
455 conversion of particulate state to the gaseous state, such as NH_4NO_3, but also conducive to
456 HNO_3 to NO_2 conversion, resulting in NO_3^- decreased and NO_2 increased.
457 In this study, SOR was obviously higher than NOR at the same particle size in the whole year,
458 indicating that the degree of oxidation of sulfate is greater than nitrogen nitrate in aerosol from
459 2004 March to 2015 February in Beibei Suburb. The NOR is considerably lower than the SOR,
460 indicating that the SOR and NOR could be the result of different ways in which sulfate- and
461 nitrate-rich particles form and the differences in their sources and removal (Zhang et al., 2011).
462
463 **4. CONCLUSION**
464 (1) Because of different meteorological factors levels in Chongqing in four seasons, some
465 differences in the size characteristics and the formation mechanisms of these ions were found.
466 SO_4^{2-} mainly distributed in the droplet mode in spring and autumn, the formation was attributed

to in-cloud processes. In summer, SO_4^{2-} distributed in the condensation mode and droplet mode, with a peak at the range of 0.43~0.65 μm, mainly was from the oxidation of SO_2 with subsequent hygroscopic growth. Except for summer, the correlation between NH_4^+ and NO_3^- was great, and mainly existed at the range of 0.65~1.10 μm in the droplet and in the form of NH_4NO_3 in aerosol. In summer, NO_3^- showed a double distribution, mainly existed in the form of $Ca(NO_3)_2$ in the coarse mode. Na^+ was a single-peak type distribution in spring and summer, but appeared a double peak type in autumn and winter. K^+ showed a single peak type in each season, mainly appeared in fine mode. The existent form of Cl^- was KCl in fine mode, and $CaCl_2$ in coarse mode. Mg^{2+}, Ca^{2+} and F^- were mainly presented in the coarse particles in the whole year. Mg^{2+} was bimodal pattern distribution in spring and summer, and less distributed in autumn and winter. The concentration of Ca^{2+} increased with particle size.

(2) There existed a certain correlation between different ions in the $PM_{2.1}$ and $PM_{9.0}$, and the cation's concentrations were significantly higher than those of anions. The correlations between Na^+, NH_4^+, K^+, Cl^-, NO_3^-, SO_4^{2-} and total water-soluble ions were stronger in $PM_{2.1}$, but the correlations between Mg^{2+}, Ca^{2+}, F^- and total water-soluble ions were stronger in $PM_{9.0}$.

(3) The emissions from motor vehicle exhaust, combustion process, soil sources and building construction dust were the major sources of the water-soluble ions in Beibei Suburb.

(4) The conversion of SO_2 and NO_2 mainly occurred in the fine particles. SOR was appeared the highest in summer and lowest in winter, but NOR in winter was higher than other seasons. SOR value of condensation-mode (0.43-0.65 μm) was greater than 0.10 only in summer, indicating that SO_4^{2-} in summer was mainly from the oxidation of SO_2 with subsequent hygroscopic growth. Higher SO_4^{2-} accompanied lower SOR in winter indicated that the sources might mainly come from the long range transportation, resulting in the heterogeneous reaction of SO_2. NOR in summer was the lowest that probably caused by temperature and photochemical reaction. SOR was considerably higher than NOR at the same particle size in the whole year, indicating that the degree of oxidation of sulfate was greater than nitrate in aerosol from 2004 March to 2015 February in Beibei Suburb.

ACKNOWLEDGEMENTS

This study was jointly supported by the Key Program of National Natural Science Foundation of China (41230642), the National Natural Science Foundation of China (41275160), the Strategic Pilot Science and Technology Project of the Chinese Academy of Sciences (XDA05100100) and the Fundamental Research Funds for the Central Universities (XDJK2015A013).

REFERENCES

Begam, G.R., Vachaspati, C.V., Ahammed, Y.N., Kumar, K.R., Reddy, R.R., Sharma, S.K., Saxena, M. and Mandal, T.K. (2016). Seasonal characteristics of water-soluble inorganic ions and carbonaceous aerosols in total suspended particulate matter at a rural semi-arid site, Kadapa (India). *Envir. Sci. Pollut. R.* 24(2): 1-16.

Cao, S., Dan, W., Chen, L.Z., Xia, J.R., Lu, J.G., Liu, G., Li, F.Y., Yang, M. (2016). Characteristics of water-soluble inorganic ions of aerosol in China. *Environ. Sci. Technol.* 39(08): 103-115.

Chen, H.H., Dui, W.U., Tan, H.B., Fei, L.I. and Fan, S.J. (2010). Study on the character of haze weather process from the year 2001 to 2008 over the Pearl River Delta. *J. Trop. Meteorol*. 26: 147-155.

Chen, J., Qiu, S.S., Shang, J., Wilfrid, O.M.F., Liu, X.G., Tian, H.Z., Boman, J. (2014). Impact of relative humidity and water soluble constituents of $PM_{2.5}$ on visibility impairment in Beijing, China. *Aerosol Air Qual. Res.* 14(1): 260-268.

Chen, L.W., Chow, J.C., Doddridge, B.G., Dickerson, R.R., Ryan, W.F. and Mueller, P.K. (2003). Analysis of a summertime $PM_{2.5}$ and haze episode in the Mid-Atlantic region. *J. Air. Waste Manage*. 53: 946.

Chen, W.H., Wang, X.M., Cohen, J.B., Zhou, S.Z., Zhang, Z.S., Chang, M., Chan, C.Y. (2016). Properties of aerosols and formation mechanisms over southern China during the monsoon season. *Atmos. Chem. Phys.* 16: 13271-13289.

Chueinta, W., Hopke, P.K. and Paatero, P. (2000). Investigation of sources of atmospheric aerosol at urban and suburban residential areas in Thailand by positive matrix factorization. *Atmos. Environ*. 34: 3319-3329.

Dlugi, R., Jordan, S. and Lindemann, E. (1981). The heterogeneous formation of sulfate aerosols in the atmosphere. *J. Aerosol. Sci.* 12: 185-197.

He, K., Zhao, Q., Ma, Y., Duan, F., Yang, F., Shi, Z., Chen, G. (2012). Spatial and seasonal variability of $PM_{2.5}$ acidity at two Chinese megacities: insights into the formation of secondary inorganic aerosols. *Atmos. Chem. Phys.* 12(3): 1377-1395.

He, Q., Yan, Y., Guo, L., Zhang, Y., Zhang, G. and Wang, X. (2017). Characterization and source analysis of water-soluble inorganic ionic species in $PM_{2.5}$ in Taiyuan city, China. *Atmos. Environ*. 184: 48-55.

Henning, S., Weingartner, E., Schwikowski, M., Gäggeler, H. W., Gehrig, R., & Hinz, K. P., Trimborn, A., Spengler, B., Baltensperger, U. (2003). Seasonal variation of water-soluble ions of the aerosol at the high-alpine site jungfraujoch (3580 m asl). *J. Geophys. Res.* 108(1): ACH 8-1–ACH 8-10.

Imhof, D., Weingartner, E., Prév t, A.S.H., Ordó ez, C., Kurtenbach, R., Wiesen, P., Rodler, J., Sturm, P., McCrae, I., Ekström, M., Baltensperger, U. (2006). Aerosol and nox emission factors and submicron particle number size distributions in two road tunnels with different traffic regimes. *Atmos. Chem. Phys.* 6(8): 2215-2230.

Jiang, C.T., Zhang, D., Zheng, J.J. (2009). Water soluble ions of PM_{10} in Chongqing. *Environ. Sci. Technol.* 32(7): 109-112. (in Chinese with English abstract)

John, W., Wall, S.M., Ondo, J.L., Winklmayr, W., 1990. Modes in the size distributions of atmospheric inorganic aerosol. *Atmos. Environ*. 24A: 2349-2359.

Li, X.R., Wang, L.L., Ji, D.S., Wen, T.X., Pan, Y.P., Sun, Y., Wang, Y.S. (2013). Characterization of the size-segregated water-soluble inorganic ions in the Jing-Jin-Ji urban agglomeration: Spatial/temporal variability, size distribution and sources. *Atmos. Environ*. 77(7): 250-259.

Liu, Z., Xie, Y.Z., Hu, B., Wen, T.X., Xin, J.Y., Li, X.R., Wang, Y.S. (2017). Size-resolved aerosol water-soluble ions during the summer and winter seasons in Beijing: formation mechanisms of secondary inorganic aerosols. *Chemosphere.* 183: 119-131.

Li, Z.Y., Liu, Y.S., Lin, Y.J., Gautam, S.H., Kuo, H.C., Tsai, C.J., Yeh, H.J., Huang, W., Li, S.W., Wu, G.J. (2017). Development of an automated system (PPWD/PILS) for studying $PM_{2.5}$ water-soluble ions and precursor gases: field measurements in two cities, Taiwan. *Aerosol Air Qual. Res.* 17(2): 1-18.

Meng, Z., Seinfeld, J.H., 1994. On the source of the submicrometer droplet mode of urban and regional aerosols. *Aerosol Sci. Tech.* 20: 253-265.

Ohta, S., Okita, T. (1990). A chemical characterization of atmospheric aerosol in Sapporo. *Atmos. Environ*. 24(4): 815-822.

Pakkanen, T.A., Kerminen, V.M., Hillamo, R.E., Makinen, M., Makela, T., Virkkula, A., 1996. Distribution of nitrate over sea-salt and soil derived particles—implications from a field study. *J. Atmos. Chem.* 24: 189-205.

Parmar, R.S., Satsangi, G.S., Kumari, M., Lakhani, A., Srivastava, S.S., Prakash, S. (2001). Study of size distribution of atmospheric aerosol at Agra. *Atmos. Environ*. 35(4): 693-702.

Satsangi, A., Pachauri, T., Singla, V., Lakhani, A., K. Kumari, K.M. (2013). Water soluble ionic species in atmospheric aerosols: concentrations and sources at Agra in the Indo-Gangetic Plain (IGP). *Aerosol Air Qual. Res.* 13(6): 1877-1889.

Seinfeld, J.H., Pandis, S.N. (2006). Atmospheric Chemistry and Physics: from Air Pollution to Climate Change, second ed. John Willey & Sons, Inc., New York.

Shen, Z.X., Zhang, L.M., Cao, J.J., Tian, J., Liu, L., Wang, G.H., Zhao, Z.Z., Wang, X., Zhang, R.J., and Liu, S.X. (2012). Chemical composition, sources, and deposition fluxes of water-soluble inorganic ions

564 obtained from precipitation chemistry measurements collected at an urban site in northwest China. *J.*
565 *Environ. Monitor.* 14: 3000-3008.
566 Sorooshian, A., Shingler, T., Harpold, A., Feagles, C.W., Meixner, T., Brooks, PD. (2013). Aerosol and
567 precipitation chemistry in the Southwestern United States: spatiotemporal trends and
568 interrelationships. *Atmos. Chem. Phys.* 13(15): 8615-8662.
569 Su, J., Zhao, P.S., Dong, Q. (2017). Chemical compositions and liquid water content of size-resolved aerosol in
570 Beijing. *Aerosol Air Qual. Res.* DOI: 10.4209/aaqr.2017.03.0122
571 Sun, Y.L., Zhuang, G.S., Tang, A.H. Wang, Y., An, Z. (2006). Chemical characteristics of $PM_{2.5}$ and PM_{10} in
572 haze_fog episodes in Beijing. *Envir. Sci. Pollut. R.* 40(10): 3148-3155.
573 Suzuki, I., Hayashi, K., Igarashi, Y., Takahashi, H., Sawa, Y., Ogura, N., Akagi, T. and Dokiya, Y. (2008).
574 Seasonal variation of water-soluble ion species in the atmospheric aerosols at the summit of Mt. Fuji.
575 *Atmos. Environ.* 42: 8027-8035.
576 Szopa, S., Balkanski, Y., Schulz, M., Bekki, S., Cugnet, D., Fortems-Cheiney, A., Turquety, S., Cozic, A.,
577 Déandreis, C. and Hauglustaine, D. (2013). Aerosol and ozone changes as forcing for climate evolution
578 between 1850 and 2100. *Clim. Dynam*. 40: 2223-2250.
579 Tang, A.H., Zhuang, G.S., Wang, Y., Yuan, H., Sun, Y.L. (2005). The chemistry of precipitation and its relation
580 to aerosol in Beijing. *Atmos. Environ*. 39(19): 3397-3406.
581 Tao, Y., Yin, Z., Ye, X.N., Ma, Z., Chen, J.M. (2014). Size distribution of water-soluble inorganic ions in urban
582 aerosols in Shanghai. *Atmos. Pollut. Res.* 5(4): 639-647.
583 Tian, M., Wang, H.B., Chen, Y., Zhang, L.M., Shi, G.M., Liu, Y., Yu, J.Y., Zhai, C.Z., Wang, J., Yang, F.M.
584 (2016). Highly time-resolved characterization of water-soluble inorganic ions in $PM_{2.5}$ in a humid and
585 acidic mega city in Sichuan Basin, China. *Sci. Total Environ.* 580: 224-234.
586 Tian, S.L., Pan, Y.P., Wang, Y.S., 2016a. Size-resolved source apportionment of particulate matter in urban
587 Beijing during haze and non-haze episodes. *Atmos. Chem. Phys.* 16: 1-19.
588 Kerminen, V., Anttila, T., Lehtinen, K. & Kulmala, M. (2011). Parameterization for atmospheric new-particle
589 formation: application to a system involving sulfuric acid and condensable water-soluble organic vapors.
590 *Aerosol Sci. Tech.* 38(10): 1001-1008.
591 Wan, X., Kang, S.C., Xin, J.J., Liu, B., Wen, T.X., Wang, P.L., Wang, Y.S., Cong, Z.Y. (2016). Chemical
592 composition of size-segregated aerosols in Lhasa city, Tibetan Plateau. *Atmos. Res.* 174-175:142-150.
593 Wang, H. and Shooter, D. (2001). Water soluble ions of atmospheric aerosols in three New Zealand cities:
594 Seasonal changes and sources. *Atmos. Environ*. 35: 6031-6040.
595 Wang, Y., Zhuang, G., Tang, A. (2005). The ion chemistry and the source of $PM_{2.5}$ aerosol in Beijing. *Atmos.*
596 *Environ*. 39(21): 3771-3784.

Wang, Y., Zhuang, G.S., Sun, Y.L., An, Z. (2005). Water-soluble part of the aerosol in the dust storm season-evidence of the mixing between mineral and pollution aerosol. *Atmos. Environ*. 39(37): 7020-7029.

Wang, H., Zhu, B., Shen, L., Xu, H., An, J., Xue, G. and Cao, J. (2015). Water-soluble ions in atmospheric aerosols measured in five sites in the Yangtze River Delta, China: Size-fractionated, seasonal variations and sources. *Atmos. Environ*. 123: 370-379.

Wang, L., Ji, D.S., Li,Y., Gao, M., Tian, S.L., Wen,T.X., Liu, Z.R., Wang, L.L., Xu, P., Jiang, C.S., Wang,Y.S. (2017). The impact of relative humidity on the size distribution and chemical processes of major water-soluble inorganic ions in the megacity of Chongqing, China. *Atmos. Res.* 192: 19-29.

Wu, X., Deng, J.J., Chen, J.S., Hong, Y.W., Xu, L.L., Yin, L.Q., Du, W.J., Hong, Z.Y., Dai, N.Z., Yuan, C.S. (2017). Characteristics of water-soluble inorganic components and acidity of $PM_{2.5}$ in a coastal city of China. *Aerosol Air Qual. Res.* 17: 2152-2164.

Xu, L., Chen, X., Chen, J., Zhang, F., He, C., Zhao, J. and Yin, L. (2012). Seasonal variations and chemical compositions of $PM_{2.5}$ aerosol in the urban area of Fuzhou, China. *Atmos. Res*. 104-105: 264-272.

Yang, Y.Y., Zhou, R., Wu, J.J., Yu, Y., Ma, Z.Q., Zhang, L.J., Di, Y.A. (2015). Seasonal variations and size distributions of water-soluble ions in atmospheric aerosols in Beijing, 2012. *J. Environ. Sci.* 34(8): 197-205.

Yue, D.L., Zhong, L.L., Zhang, T., Shen, J., Yuan, L., Ye, S.Q., Zhou, Y., Zeng, L.M. (2016). Particle growth and variation of cloud condensation nucleus activity on polluted days with new particle formation: a case study for regional air pollution in the PRD region, China. *Aerosol Air Qual. Res.* 16: 323-335.

Zhang, T., Cao, J.J., Tie, X.X., Shen, Z.X., Liu, S.X., Ding, H., Han, Y.M., Wang, G.H., Ho, K.F. and Qiang, J. (2011). Water-soluble ions in atmospheric aerosols measured in Xi'an, China: Seasonal variations and sources. *Atmos. Res.* 102: 110-119.

Zhou, Y., Fu, J.S., Zhuang, G., Levy, J.I. (2010). Risk-based prioritization among air pollution control strategies in the Yangtze River Delta, China. *Environ. Health Persp.* 118: 1204-1210.

Zhuang, H, Chan, C.K., Fang, M., Wexler, A.S. 1999. Formation of nitrate and non-sea-salt sulfate on coarse particles. *Atmos. Environ*. 33: 4223-4233.

Figure legends:

Fig. 1 A sky view of sampling site in the urban area of Beibei (29°48'43″N, 106°24'58″E), Chongqing, China

Fig. 2 Size distributions of water-soluble ions in the aerosol in spring in the urban area of Beibei

Fig. 3 Size distributions of water-soluble ions in the aerosol in summer in the urban area of Beibei

Fig. 4 Size distributions of water-soluble ions in the aerosol in autumn in the urban area of Beibei

Fig. 5 Size distributions of water-soluble ions in the aerosol in winter in the urban area of Beibei

Fig. 6 Size distributions of apparent conversion rate (SOR and NOR) in each season

Table legends:

Table 1 The meteorological parameters and atmospheric pollutants during four seasons

Table 2 Correlation coefficients matrix for the concentrations of water-soluble ions in $PM_{2.1}$

Table 3 Correlation coefficients matrix for the concentrations of water-soluble ions in $PM_{9.0}$

Table 4 The results of factor analysis for water-soluble ions in $PM_{2.1}$ and $PM_{9.0}$

Table 1 The meteorological parameters and atmospheric pollutants during four seasons

Parameter	Spring	Summer	Autumn	Winter
Sunshine hours (h)	126	326.7	121.1	64.2
Ly Wind speed (m/s)	13.77	13.57	12.09	12.70
Air temperature (°C)	18.47	27.16	19.70	10.24
Relative humidity (%)	77.98	75.66	82.97	78.31
Precipitation (mm)	418.2	598.7	394.9	49.5
SO_2 ($\mu g \cdot m^{-3}$)	28.5	15.1	16.3	34.4
NO_2 ($\mu g \cdot m^{-3}$)	36.5	31.5	39.0	40.8
O_3 ($\mu g \cdot m^{-3}$)	37.1	58.8	26.9	15.6

Table 2 Correlation coefficients matrix for the concentrations of water-soluble ions in $PM_{2.1}$

	Na^+	NH_4^+	K^+	Mg^{2+}	Ca^{2+}	F^-	Cl^-	NO_3^-	SO_4^{2-}	Σ(+)	Σ(-)
Na^+	1.00	0.37*	0.14	0.10	0.18	0.21	0.35*	0.35*	0.53**	0.44**	0.51**
NH_4^+		1.00	0.64**	0.13	0.06	0.22	0.76**	0.91**	0.82**	0.99**	0.94**
K^+			1.00	0.18	0.23	0.19	0.54**	0.71**	0.51**	0.68**	0.65**
Mg^{2+}				1.00	0.41**	0.25	0.07	0.24	0.23	0.21	0.25
Ca^{2+}					1.00	0.28	0.21	0.05	0.21	0.18	0.17
F^-						1.00	0.21	0.15	0.39**	0.27	0.34*
Cl^-							1.00	0.70**	0.49**	0.78**	0.68**
NO_3^-								1.00	0.66**	0.91**	0.87**
SO_4^{2-}									1.00	0.84**	0.94**
Σ(+)										1.00	0.96**
Σ(-)											1.00

Note: * represents significant correlation (P<0.05) , ** represents highly significant correlation (P<0.01).

Table 3 Correlation coefficients matrix for the concentrations of water-soluble ions in $PM_{9.0}$

	Na^+	NH_4^+	K^+	Mg^{2+}	Ca^{2+}	F^-	Cl^-	NO_3^-	SO_4^{2-}	Σ(+)	Σ(-)
Na^+	1.00	0.20	0.02	0.13	0.04	0.10	0.22	0.24	0.38*	0.28	0.34*
NH_4^+		1.00	0.57**	0.08	0.26	0.52**	0.57**	0.89**	0.79**	0.87**	0.89**
K^+			1.00	0.11	0.32*	0.55**	0.43**	0.68**	0.50**	0.59**	0.63**
Mg^{2+}				1.00	0.47**	0.19	0.50**	0.16	0.17	0.37*	0.24
Ca^{2+}					1.00	0.49**	0.31*	0.37*	0.39**	0.68**	0.43**
F^-						1.00	0.67**	0.55**	0.53**	0.63**	0.64**
Cl^-							1.00	0.57**	0.46**	0.62**	0.64**
NO_3^-								1.00	0.75**	0.86**	0.91**
SO_4^{2-}									1.00	0.81**	0.94**
Σ(+)										1.00	0.90**
Σ(-)											1.00

Note: * represents significant correlation (P<0.05) , ** represents highly significant correlation (P<0.01).

Table 4 The results of factor analysis for water-soluble ions in $PM_{2.1}$ and $PM_{9.0}$

Ion component	$PM_{2.1}$		$PM_{9.0}$		
	Factor 1	Factor 2	Factor 1	Factor 2	Factor 3
Na^+	0.521	0.097	0.299	-0.069	0.890
NH_4^+	0.925	-0.283	0.852	-0.359	0.007
K^+	0.745	-0.098	0.722	-0.187	-0.350
Mg^{2+}	0.316	0.678	0.365	0.815	0.179
Ca^{2+}	0.298	0.739	0.554	0.531	-0.189
F^-	0.389	0.515	0.769	0.114	-0.233
Cl^-	0.789	-0.189	0.760	0.276	0.070
NO_3^-	0.892	-0.257	0.892	-0.268	-0.020
SO_4^{2-}	0.846	0.033	0.829	-0.227	0.197
Variance contribution rate (%)	46.161	16.365	49.233	14.762	12.016
Cumulative variance contribution rate (%)	46.161	62.526	49.233	63.995	76.011

Table 1 The meteorological parameters and atmospheric pollutants during four seasons

Parameter	Spring	Summer	Autumn	Winter
Sunshine hours (h)	126	326.7	121.1	64.2
Ly Wind speed (m/s)	13.77	13.57	12.09	12.70
Air temperature (°C)	18.47	27.16	19.70	10.24
Relative humidity (%)	77.98	75.66	82.97	78.31
Precipitation (mm)	418.2	598.7	394.9	49.5
SO_2 ($\mu g \cdot m^{-3}$)	28.5	15.1	16.3	34.4
NO_2 ($\mu g \cdot m^{-3}$)	36.5	31.5	39.0	40.8
O_3 ($\mu g \cdot m^{-3}$)	37.1	58.8	26.9	15.6

Table 2 Correlation coefficients matrix for the concentrations of water-soluble ions in $PM_{2.1}$

	Na^+	NH_4^+	K^+	Mg^{2+}	Ca^{2+}	F^-	Cl^-	NO_3^-	SO_4^{2-}	Σ(+)	Σ(-)
Na^+	1.00	0.37*	0.14	0.10	0.18	0.21	0.35*	0.35*	0.53**	0.44**	0.51**
NH_4^+		1.00	0.64**	0.13	0.06	0.22	0.76**	0.91**	0.82**	0.99**	0.94**
K^+			1.00	0.18	0.23	0.19	0.54**	0.71**	0.51**	0.68**	0.65**
Mg^{2+}				1.00	0.41**	0.25	0.07	0.24	0.23	0.21	0.25
Ca^{2+}					1.00	0.28	0.21	0.05	0.21	0.18	0.17
F^-						1.00	0.21	0.15	0.39**	0.27	0.34*
Cl^-							1.00	0.70**	0.49**	0.78**	0.68**
NO_3^-								1.00	0.66**	0.91**	0.87**
SO_4^{2-}									1.00	0.84**	0.94**
Σ(+)										1.00	0.96**
Σ(-)											1.00

Note: * represents significant correlation (P<0.05) , ** represents highly significant correlation (P<0.01).

Table 3 Correlation coefficients matrix for the concentrations of water-soluble ions in $PM_{9.0}$

	Na^+	NH_4^+	K^+	Mg^{2+}	Ca^{2+}	F^-	Cl^-	NO_3^-	SO_4^{2-}	Σ(+)	Σ(-)
Na^+	1.00	0.20	0.02	0.13	0.04	0.10	0.22	0.24	0.38*	0.28	0.34*
NH_4^+		1.00	0.57**	0.08	0.26	0.52**	0.57**	0.89**	0.79**	0.87**	0.89**
K^+			1.00	0.11	0.32*	0.55**	0.43**	0.68**	0.50**	0.59**	0.63**
Mg^{2+}				1.00	0.47**	0.19	0.50**	0.16	0.17	0.37*	0.24
Ca^{2+}					1.00	0.49**	0.31*	0.37*	0.39**	0.68**	0.43**
F^-						1.00	0.67**	0.55**	0.53**	0.63**	0.64**
Cl^-							1.00	0.57**	0.46**	0.62**	0.64**
NO_3^-								1.00	0.75**	0.86**	0.91**
SO_4^{2-}									1.00	0.81**	0.94**
Σ(+)										1.00	0.90**
Σ(-)											1.00

Note: * represents significant correlation (P<0.05) , ** represents highly significant correlation (P<0.01).

Table 4 The results of factor analysis for water-soluble ions in $PM_{2.1}$ and $PM_{9.0}$

Ion component	$PM_{2.1}$		$PM_{9.0}$		
	Factor 1	Factor 2	Factor 1	Factor 2	Factor 3
Na^+	0.521	0.097	0.299	-0.069	0.890
NH_4^+	0.925	-0.283	0.852	-0.359	0.007
K^+	0.745	-0.098	0.722	-0.187	-0.350
Mg^{2+}	0.316	0.678	0.365	0.815	0.179
Ca^{2+}	0.298	0.739	0.554	0.531	-0.189
F^-	0.389	0.515	0.769	0.114	-0.233
Cl^-	0.789	-0.189	0.760	0.276	0.070
NO_3^-	0.892	-0.257	0.892	-0.268	-0.020
SO_4^{2-}	0.846	0.033	0.829	-0.227	0.197
Variance contribution rate (%)	46.161	16.365	49.233	14.762	12.016
Cumulative variance contribution rate (%)	46.161	62.526	49.233	63.995	76.011

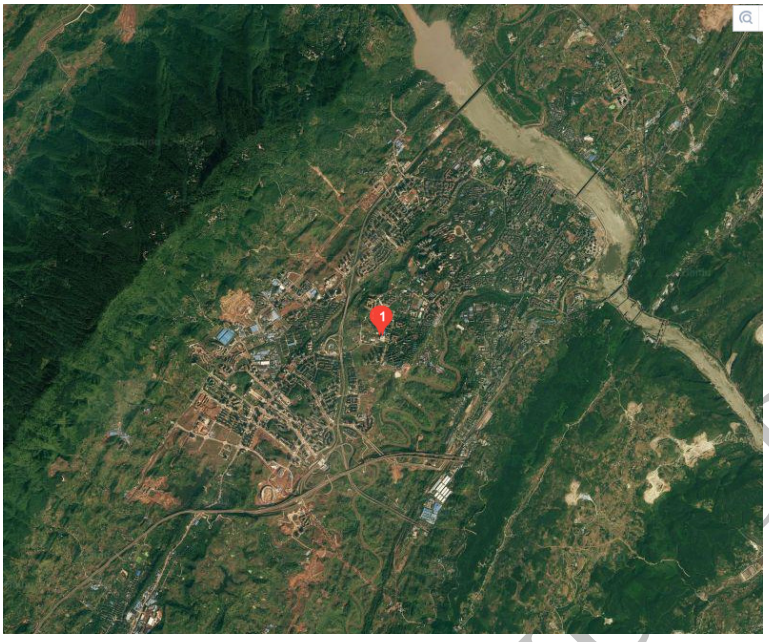

Fig. 1 A sky view of sampling site in the urban area of Beibei (29°48'43″N, 106°24'58″E), Chongqing, China

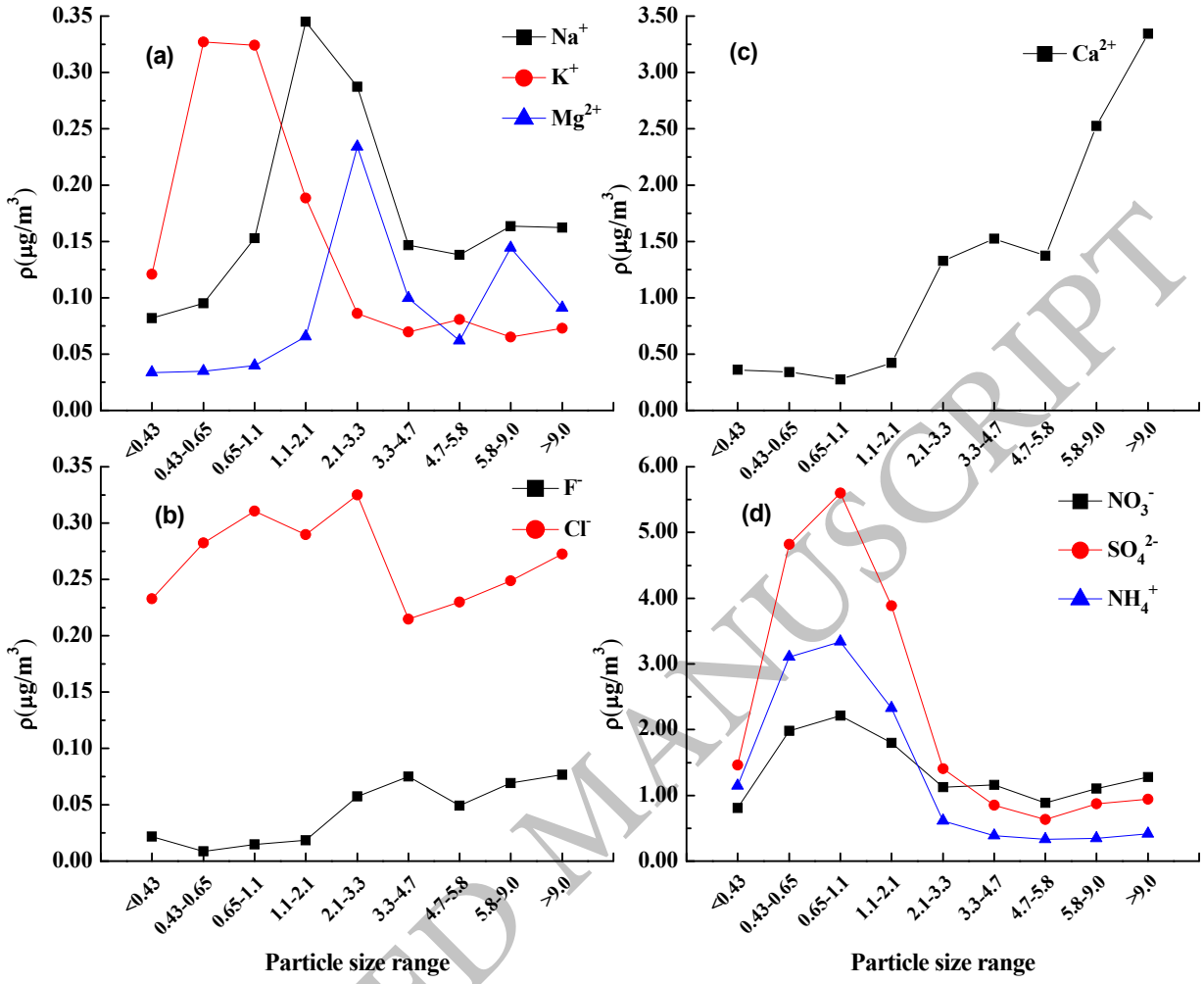

Fig. 2 Size distributions of water-soluble ions in the aerosol in spring in the urban area of Beibei

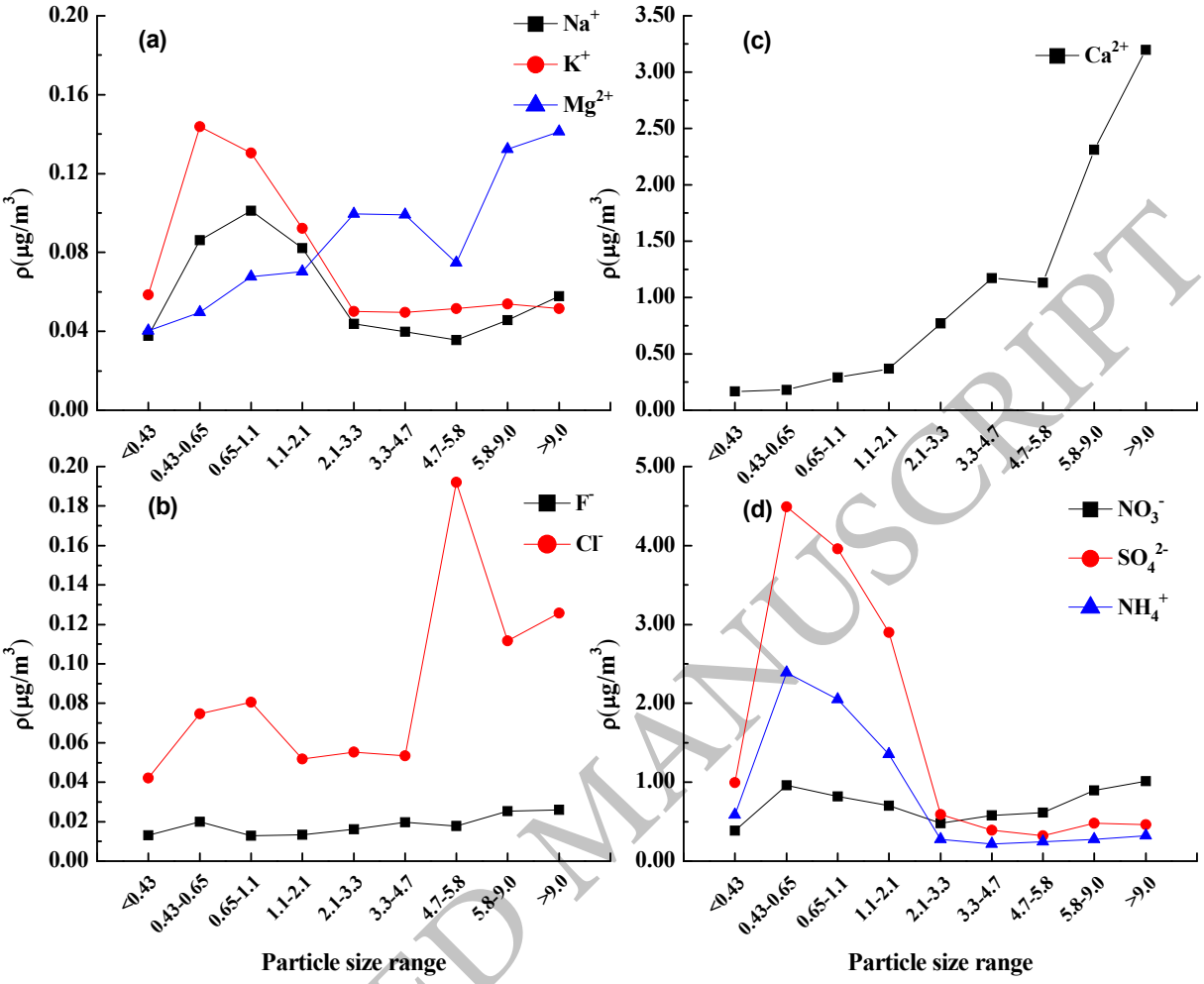

Fig. 3 Size distributions of water-soluble ions in the aerosol in summer in the urban area of Beibei

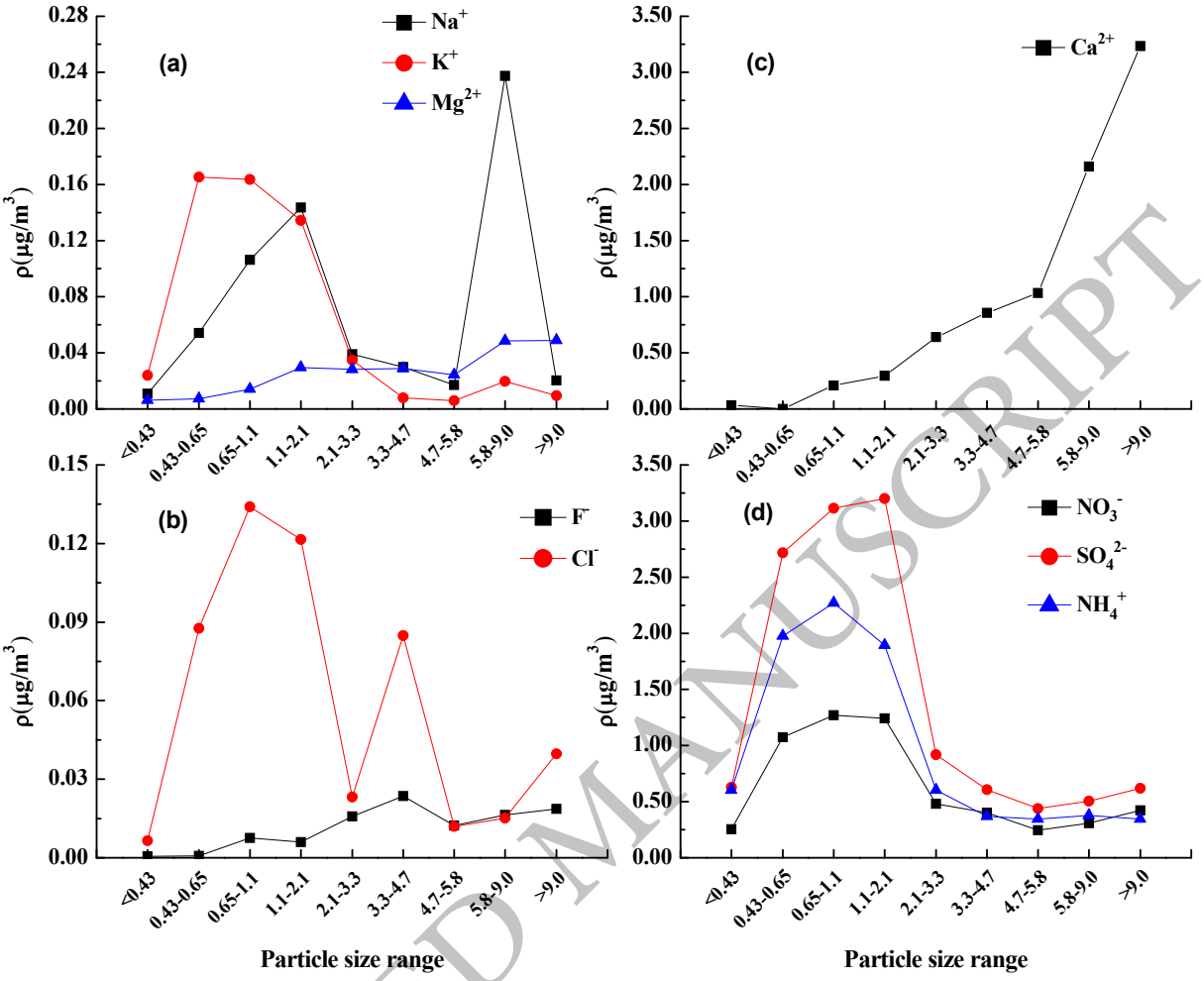

Fig. 4 Size distributions of water-soluble ions in the aerosol in autumn in the urban area of Beibei

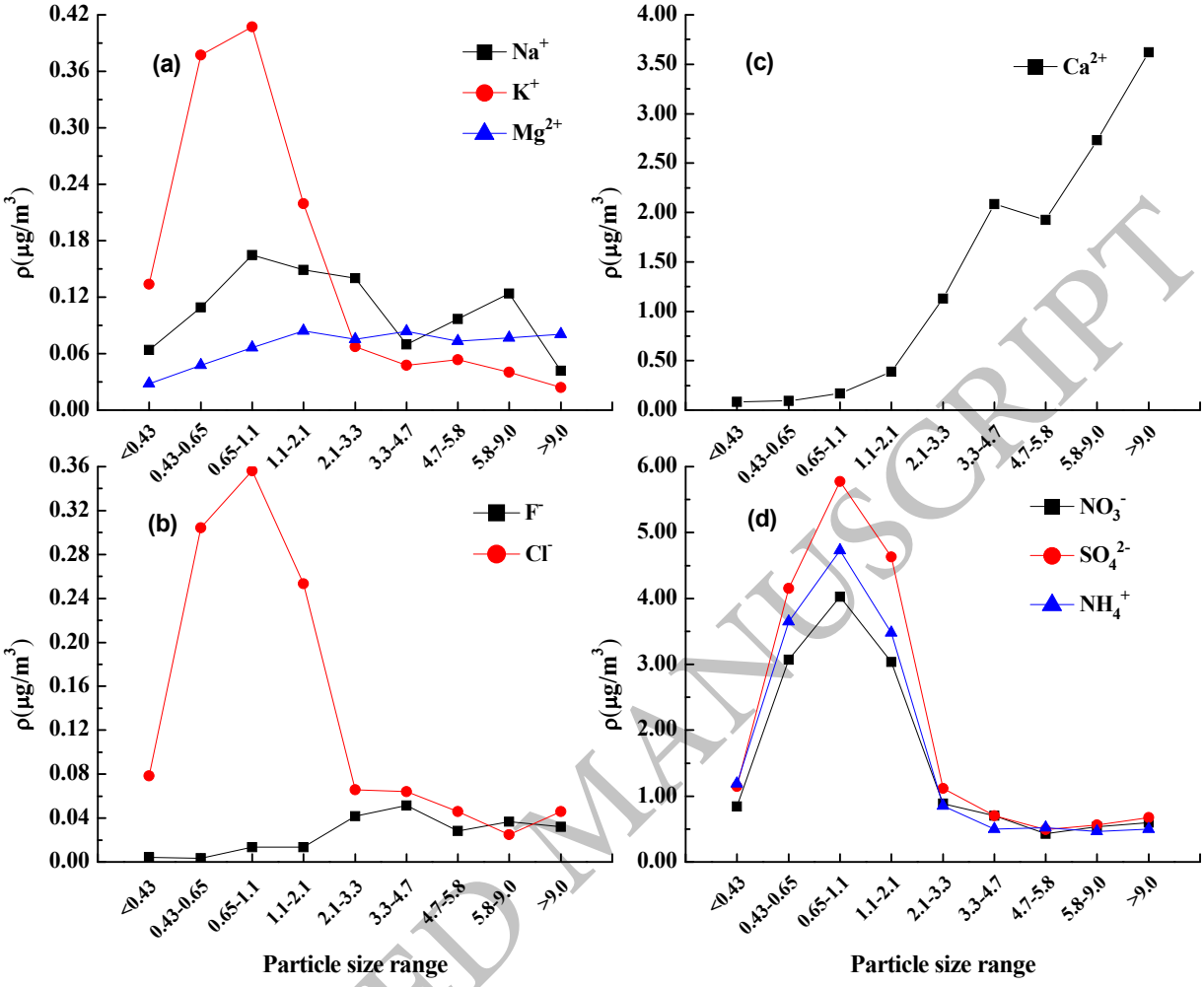

Fig. 5 Size distributions of water-soluble ions in the aerosol in winter in the urban area of Beibei

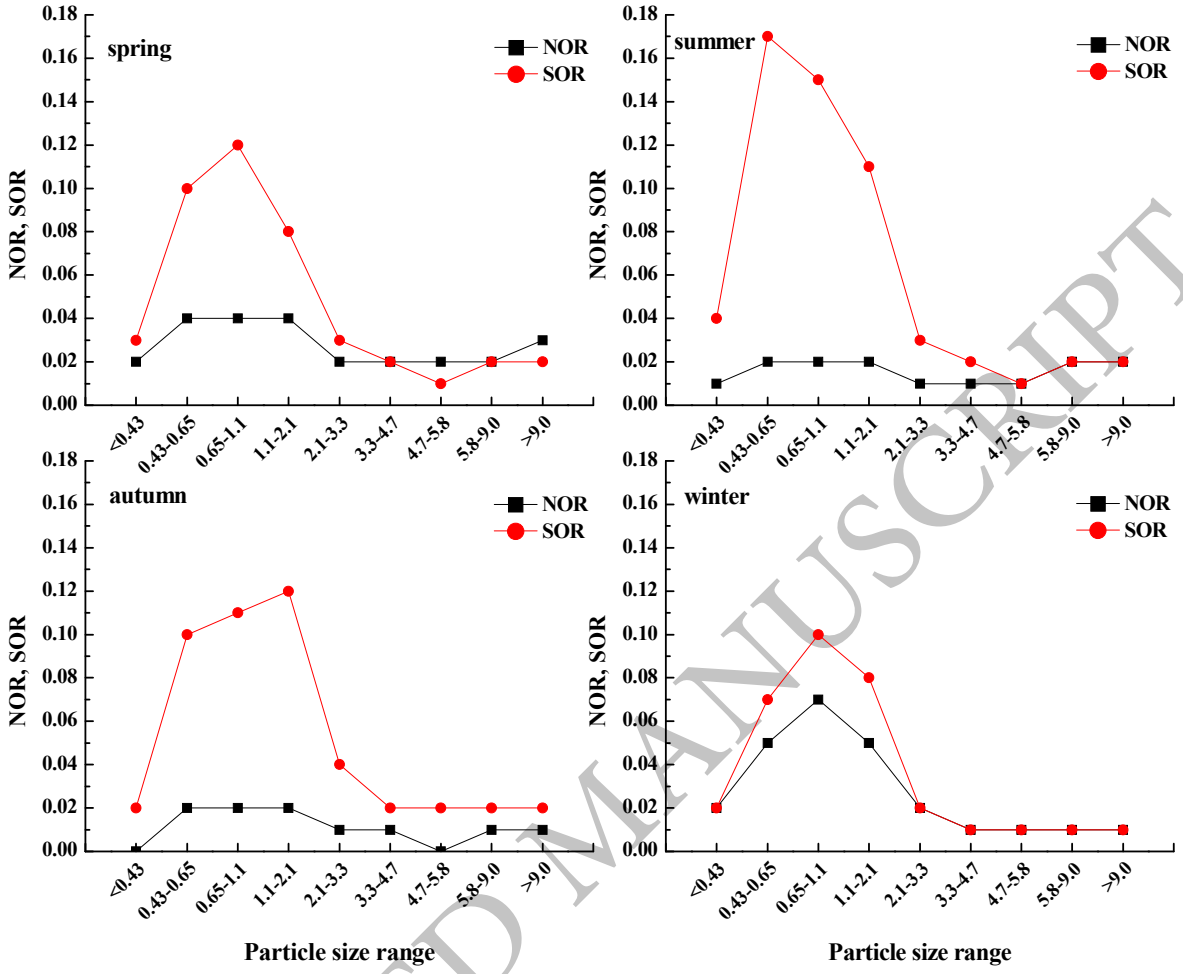

Fig. 6 Size distributions of apparent conversion rate (SOR and NOR) in each season